

# Worldwide Techniques for Predicting the Multipath Fading Distribution on Terrestrial LOS Links: Background and Results of Tests

Roderic L. Olsen, *Member, IEEE*, and Terje Tjelta

**Abstract**—In 1988, the International Telecommunication Union (ITU) adopted new methods for predicting the deep-fading distribution due to multipath propagation for the average worst month on ultra high-frequency (UHF)-super highway frequency (SHF) terrestrial line-of-sight (LOS) links. Employing refractivity gradient statistics available from world maps, the methods were recommended for application in all regions of the world. One method for the deep-fading range did not utilize detailed path profile information and was designed for preliminary planning or licensing purposes. A second method, which did employ the path profile was intended for more detailed design purposes. A multipath fading data base comprising some 246 links (including 34 over water) in 23 countries of the world has now been assembled for testing and revising these methods. Revisions to the geoclimatic model used in both methods and an associated method for predicting the shallow-fading distribution have recently been adopted by Study Group 3 of the new radiocommunications sector of the ITU (ITU-R). This paper summarizes the basis of the original and revised versions of the deep-fading prediction methods and presents the results of the most extensive tests to date. Some discussion of potential future revisions is also provided.

**Index Terms**—Fading channels, microwave radio propagation, multipath channels, prediction methods, radio repeaters.

## I. INTRODUCTION

THE extensive use of digital microwave radio links in the communications networks of various countries over the last 15 years has resulted in a renewed interest in methods of predicting the effects of multipath fading. Although emphasis has shifted somewhat to studies of wide-band effects such as distortion, there has remained a strong interest in the development of accurate methods for predicting the multipath fading distribution in a narrow frequency band (sometimes referred to as “single-frequency” methods) under varying climatic conditions. In fact, narrow-band prediction techniques are necessary elements of virtually all techniques for predicting the outage of digital links [1]. As distortion has been reduced through the use of improved equalization techniques, this narrow-band element in outage prediction has been gaining in importance. Currently, the narrow-band fading distribution is the most widely available multipath fading statistic and,

therefore, the one most suitably characterized in terms of climatic conditions.

Techniques for predicting the deep-fading range of the multipath fading distribution for the average worst month have been available for many years [2]. Most of these have been based on empirical fits of Rayleigh-type distributions (i.e., with slopes of 10 dB/decade) to the fading data for individual countries. The best known techniques in this category are those of Morita [3] for Japan (actually more a worst-season technique), Barnett [4] and Vigants [5] for the United States, Pearson [6] and Doble [7] for the United Kingdom, Nadenenko [8] for the former Soviet Union, and that of the International Radio Consultative Committee (CCIR) [9] for “Northwest” Europe. The technique of Boithias [10], [11], although designed for shallow as well as deep fading and conforming to a Rice–Nakagami distribution rather than Rayleigh-type distributions, was also fitted to fading data for “Northwest” Europe. Although these techniques have been used to varying extent in other parts of the world, link designers in other countries have been faced with the difficulty of choosing among techniques sometimes giving vastly different results for the same apparent climatic region.

To overcome this problem, in 1988 Study Group 5 of the CCIR adopted two “worldwide” techniques for predicting the deep-fading range of the multipath fading distribution [12]. Method 1 did not require detailed path profile information and was specified as best suited for preliminary planning or licensing purposes. It needed only path length, frequency, and path inclination as input variables. Method 2 did require the path profile in order to obtain an additional link variable (the “average” grazing angle of the wave specularly reflected from the ground), and was specified as more appropriate for link design. Although the methods were based only on fading data for France and the U.K. [2] and fading and refractivity gradient data for Canada [13], [14], they were specified for worldwide application because the utilization of a somewhat general procedure involving world maps of refractivity gradient statistics [15], [16] to obtain the geoclimatic factors suggested approximate worldwide applicability. Indeed, limited tests using data for a few other countries around the world indicated their approximate worldwide applicability [17]. In 1990, an interpolation procedure was introduced extending these predictions for the deep-fading range to shallow fade depths [9].

By 1993, data for 238 links (including 31 over water) in 22 countries around the world had been assembled for testing

Manuscript received April 29, 1996; revised March 11, 1997.

R. L. Olsen is with the Communications Research Centre, Department of Industry, Ottawa, Canada, K2H8S2.

T. Tjelta is with Telenor Research and Development, N-2007, Kjeller, Norway.

Publisher Item Identifier S 0018-926X(99)02475-8.

prediction procedures [18]. Several revisions to the geoclimatic factor model used in CCIR Methods 1 and 2 (and consequently in the shallow-fading procedure) were made by the new ITU-R as a result [19]. Unfortunately, the background and testing results on both the original and revised methods are not as yet well known outside ITU-R Study Group 3 (formed from previous Study Groups 5 and 6). It is the aim of this paper to provide the background in a manner that may facilitate inputs from a wider community to future revisions.

For ease of understanding the background and assessing the testing results, a summary of the original and revised versions of Methods 1 and 2 is given in Section II. The basis of the methods with the original geoclimatic factor model is provided in Section III. Testing procedures and results for the original and revised versions of Methods 1 and 2 are given in Section IV, discussion of results and the basis of the revisions in Section V. Finally, Section VI presents a summary and conclusions.

In 1992, a complementary method was adopted by the CCIR [20] for predicting the enhancement part of the overall distribution. The basis of this method is described elsewhere [21]. More recently, a method for converting the average worst-month distributions to distributions for the average year was also adopted by the ITU-R [19].

## II. SUMMARY OF THE ITU-R METHODS FOR THE DEEP-FADING RANGE

ITU-R Method 1 for predicting the deep-fading range of the multipath fading distribution requires knowledge of only three link variables: path length  $d$  (km), frequency  $f$  (GHz), and the magnitude of the path inclination  $|\varepsilon_p|$  (mrad). Method 2 requires the additional link variable  $\phi$  (mrad), which is the "average" grazing angle corresponding to a 4/3-earth radius model for refraction. The basic prediction equations (1) and (5) below are the same in both the original and revised versions of the methods (see Section III for the basis of these equations). However, the revised methods contain a more accurate set of equations for determining the geoclimatic factor  $K$ , which better takes into account the variability of climate and terrain. In the following summary of Methods 1 and 2, both the original [9], [12], [20] and revised [19] equations for the geoclimatic factor are given to facilitate the later discussion of results:

The percentage of time  $p$  that fade depth  $A$  (dB) is exceeded in the average worst month is obtained in Method 1 from the power-law expression

$$p = K d^{3.6} f^{0.89} (1 + |\varepsilon_p|)^{-1.4} \cdot 10^{-A/10} \quad (\%) \quad (1)$$

The magnitude of the path inclination required here is calculated from

$$|\varepsilon_p| = 1000 \operatorname{Arctan} [ |h_r - h_e| / 1000d ] \approx |h_r - h_e| / d \quad (\text{mrad}) \quad (2)$$

where  $h_e$  and  $h_r$  are, respectively, the heights (meters) of the transmitter and receiver above mean sea level. Although not expressed explicitly by the ITU-R, the fade depth  $A$  exceeded for  $p$  percent of the time in the average worst month can be

obtained from

$$A = G - 57 + 36 \log d + 8.9 \log f - 14 \log(1 + |\varepsilon_p|) - 10 \log p \quad (\text{dB}). \quad (3)$$

Here,  $G$  is the "logarithmic geoclimatic factor" given in terms of the geoclimatic factor  $K$  by

$$G = 10 \log K + 57 \quad (\text{dB}). \quad (4)$$

The procedure for obtaining  $K$  is discussed below. Another logarithmic geoclimatic factor  $G_E = G - 8$  dB was used previously in relation to European data [2]. The Canadian definition [14] is employed here for simplicity in the later discussion.

The corresponding basic prediction expressions for Method 2 are

$$p = K d^{3.3} f^{0.93} (1 + |\varepsilon_p|)^{-1.1} \phi^{-1.2} \cdot 10^{-A/10} \quad (\%) \quad (5)$$

$$A = G - 46 + 33 \log d + 9.3 \log f - 11 \log(1 + |\varepsilon_p|) - 12 \log \phi - 10 \log p \quad (\text{dB}) \quad (6)$$

with

$$G = 10 \log K + 46 \quad (\text{dB}). \quad (7)$$

The "average" grazing angle  $\phi$  in (5) and (6) is obtained from

$$\phi = \frac{h_1 + h_2}{d} [1 - m(1 + b^2)] \quad (\text{mrad}) \quad (8)$$

where

$$m = \frac{d^2 10^3}{4a_e(h_1 + h_2)} \quad (9)$$

$$c = \frac{|h_1 + h_2|}{h_1 + h_2} \quad (10)$$

$$b = 2\sqrt{\frac{m+1}{3m}} \cos \left[ \frac{\pi}{3} + \frac{1}{3} \operatorname{Arcos} \left( \frac{3c}{2} \sqrt{\frac{3m}{(m+1)^3}} \right) \right] \quad (11)$$

with  $a_e$  the effective radius of the earth. As described in more detail elsewhere [2], [20], the variables  $h_1$  and  $h_2$  are the heights (meters) of the transmitting and receiving antennas, respectively, above the linear regression curve through the path profile as plotted on a flat earth graph. (In the original version of Method 2 [20], special procedures were specified for dealing with rough terrain. These were dropped in the revised version [19]. The tests on the original version of Method 2 presented in Section IV employ the values of  $\phi$  obtained using the full-path profiles except for 1-km exclusion intervals at the ends of a path.)

For both the original and revised versions of Methods 1 and 2, it was recommended that the geoclimatic factor  $K$  be obtained from fading data for links in the vicinity of the planned link if such data existed. However, since in most cases sufficient suitable data do not exist, prediction procedures for calculating  $K$  based on refractivity gradient statistics were recommended.

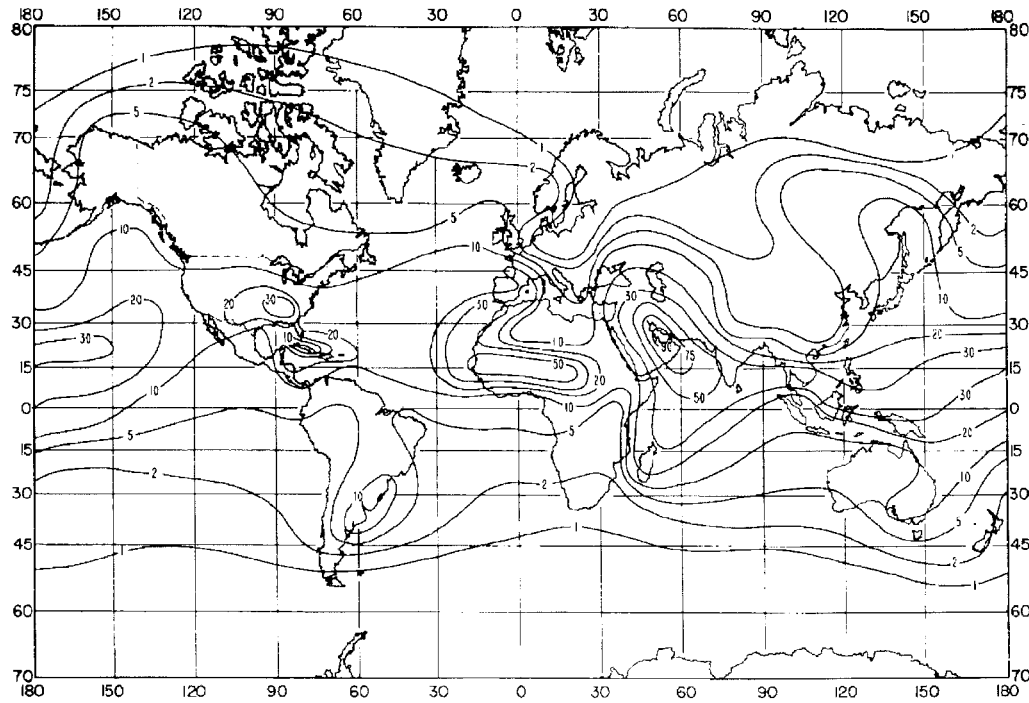


Fig. 1. Contour map of percentage of time that the refractivity gradient in the lowest 100 m of the atmosphere is more negative than  $-100$  N units/km in August (after Bean *et al.* [15]).

TABLE I

VALUES OF THE COEFFICIENT  $C_o$  IN (12) FOR VARIOUS TYPES OF LINK—ORIGINAL VERSIONS OF CCIR METHODS 1 AND 2 [20]

Type of Link	Method 1	Method 2
overland links not in mountainous regions	6.5	5.4
overland links in mountainous regions	7.1	6.0
overwater links	6.0	4.9

The prediction equations for  $K$  for the original versions of Methods 1 and 2 [9], [12], [20] can be represented by the single general equation

$$K = 10^{-C_o p_L^{1.5}} \quad (12)$$

with the values of the coefficient  $C_o$  and the conditions for their applicability summarized in Table I. The variable  $p_L$  is the percentage of time that the refractivity gradient in the lowest 100 m of the atmosphere is more negative than  $-100$  N units/km in the estimated average worst month. It is obtained by taking the highest percentage occurrence of this  $-100$  N units/km gradient from contour maps [15], [16] for four months (February, May, August, and November) representative of the four seasons. (For convenience, the map for August is reproduced in Fig. 1.) As an exception, the map for February was not to be used in the arctic.

Similarly, the prediction equations for  $K$  for the revised versions of Methods 1 and 2 [19] can be represented by

$$K = 10^{-C_o + 0.1(C_{Lat} + C_{Lon})} p_L^{1.5} \quad (13)$$

with the values of the coefficient  $C_o$  and the conditions for their applicability summarized in Table II and with the coefficient  $C_{Lat}$  of latitude  $\xi$  given by

$$C_{Lat} = 0 \quad |\xi| \leq 53^\circ \quad (14)$$

$$C_{Lat} = -53 + \xi \quad 53^\circ < |\xi| < 60^\circ \quad (15)$$

$$C_{Lat} = 7 \quad |\xi| \geq 60^\circ \quad (16)$$

and the continental longitude coefficient  $C_{Lon}$  by

$$C_{Lon} = 3 \quad \text{longitudes of Europe and Africa} \quad (17)$$

$$C_{Lon} = -3 \quad \text{longitudes of North and South America} \quad (18)$$

$$C_{Lon} = 0 \quad \text{all other longitudes.} \quad (19)$$

### III. THE BASIS OF THE METHODS AND THE ORIGINAL GEOCLIMATIC FACTOR MODEL

#### A. The Basic Models for the Tail of the Microwave Fading Distribution

Equations (1) and (5) [or (3) and (6)] are three- and four-variable models (four and five variables with the geoclimatic factor) based on microwave data for the large fade depth tail portion of the multipath fading distribution for the average worst month. The tail portion of the distribution as expressed by these equations has the Rayleigh slope of 10 dB/decade, and occurs for fade depths greater than about 15 dB on average. It is believed to be caused by a combination of atmospheric fading (largely beam spreading of the direct wave commonly referred to as defocussing) and surface reflection [2], [22], [23].

With the possible exception of minor variations discussed by Tjelta *et al.* [2], these three- and four-variable models [24] are believed to be the most accurate basic “tail” models currently available [17]. This accuracy was achieved in several ways. First of all, the models were based on a fading data base for 47 links in France and the U.K., larger than that used in the development of most earlier models [2]. No constant fade depth or probability restrictions were made in model development as previously; fade depths were chosen specifically such that they were in the distribution tails and that

TABLE II  
VALUES OF THE COEFFICIENT  $C_o$  IN (13) FOR VARIOUS TYPES OF LINK—REVISED VERSIONS OF ITU-R METHODS 1 AND 2 [19]

Type of Link	Method 1	Method 2
overland links for which the lower of the transmitting and receiving antennas is less than 700 m above mean sea level. (see Note 1 for overland links crossing small lakes and rivers)	6.5	5.4
overland links for which the lower of the transmitting and receiving antennas is higher than 700 m above mean sea level (see Note 1 for links crossing small lakes and rivers.)	7.1	6.0
links over medium-sized bodies of water (see Note 1), coastal areas beside such bodies of water (see Note 2), or regions of many lakes (see Note 4)	5.9	4.8
links over large bodies of water (see Note 1), or coastal areas beside such bodies of water (see Note 3)	5.5	4.4

they had the highest exceedance probabilities possible within this constraint so as to maximize statistical stability.

In some previous analyses, the worst one-month distributions over different measurement durations were mixed (i.e., worst-month distributions for one year were combined with those for two years, three years, etc. in the fitting). Such mixed statistics have a bias (e.g., four-year worst-month fade depths tend to be larger than three-year fade depths, etc.) and those associated with the longest overall durations of measurement have very large standard errors. The new approach [2], [24] used the average worst-month distribution envelope [25], whatever the number of years, eliminating bias.

Perhaps the greatest improvements in the new models resulted from the use of systematic correlation analyses, multiple regression, and multiple iteration [2], [24]. Multiple regression gives the most accurate relationship between the exponents in the power law and multiple iteration allows the geoclimatic factor to vary from one region to another, at the same time increasing the accuracy of the multiple regression. One major outcome of the correlation analyses is that the path inclination was found to be a more significant variable than the surface roughness variable originally introduced by Pearson [6] and later employed by Vigants [5], at least in describing link variability within regions for which the geoclimatic factor is fairly constant.

### B. Prediction of the Geoclimatic Factor Based on Refractivity Gradient Statistics

The development of the original geoclimatic factor model in (12) was carried out in several stages. The stages based on the Canadian fading and refractivity gradient data bases have been described in detail by Olsen and Segal [14] and will only be summarized here. The final stage of extending the Canadian result for global applications will be described in more detail.

*Establishment of a prediction relation and map for the geoclimatic factor in Canada:* Working backward from the prediction equation (6) developed from the British-French data, the first step was to calculate the logarithmic geoclimatic factors  $G$  corresponding to each of 29 links in the Canadian worst-month fading data base. In two reference regions of the country, the observed values of  $G$  calculated were averaged to obtain overall averages for these two regions. The approach was later cited by the CCIR/ITU-R as a way to develop geoclimatic factors for regions or countries for which sufficient data are available [19], [20].

The second step in the modeling process was to find a climatic variable that was sufficiently well correlated with the geoclimatic factor. The variable finally employed was  $p_d$ , the combined occurrence of surface and elevated surface ducts in the average worst three-month period obtained from a 47-site three-year radiosonde data base for Canada and adjacent parts of the U.S. [26].

The final step was to establish a relation between  $G$  and  $p_d$ . The most plausible relationship seemed to be a logarithmic one, as between the fade depth  $A$  (dB) and its exceedance percentage  $p$ . Thus, the “two-region” fit established from the two sets of  $G$  and  $p_d$  values for the two reference regions was

$$G = -11 + 15 \log p_d(\text{dB}). \quad (20)$$

This relation was then used to establish contours of constant  $G$  on a map of Canada and adjacent areas of the U.S. (see Fig. 3 of [14]).

*Choice of a Suitable Climatic Variable to Characterize Fading Worldwide:* Since the geoclimatic prediction variable  $p_d$  available in Canada was not available on a worldwide basis, another suitable variable had to be found to develop worldwide prediction equations for the geoclimatic factor. Since the maps of Bean *et al.* [15] used to obtain  $p_L$  were available, this variable was considered. Values of  $p_L$  were obtained from the map for August (see Fig. 1) for six locations in eastern North America where the map was known to be most accurate on the basis of the high density of radiosonde sites in the data base. A comparison with corresponding values of  $p_d$  for the average worst three-month period showed reasonable correlation with values of  $p_L$  (equal to about three quarters those of  $p_d$  on average).

*Establishment of “Worldwide” Prediction Relations for the Geoclimatic Factor in Nonmountainous Regions:* On the basis of the preceding results, it was decided to try replacing  $p_d$  in (20) by  $p_L$  and to establish a new intercept value based on the fading data available for Canada, France, and the U.K. This was done by iteratively comparing predicted values of  $G$  based on (20) with average values observed from the measurements in eastern Canada [13], [14], France, and the U.K. [2] and then adjusting the intercept to reduce the error. The final iterations for Methods 1 and 2 were reported earlier [13]. The data for eastern Canada alone were used in the fitting since it was known that the maps of Bean *et al.* [15] were most accurate in this region (because of the high density of radiosonde stations). Moreover, since it was believed that the maps were inaccurate in the East Anglia region of the U.K. (because of the low density of radiosonde stations in



Fig. 2. Map of the world showing countries for which data are available in the ITU-R data base, and the number of links for each country (246 links total).

this part of Europe and the knowledge from fading data that this small coastal region showed severe fading in relation to surrounding regions [2], [24]), this region was ignored in the fitting. The resulting prediction equations for Methods 1 and 2 are those given in (12) with the coefficients  $C_o$  of Table I for nonmountainous regions.

*“Correction Factor” for Mountainous Regions:* Initial results using (12) applied to the mountainous regions of British Columbia compared with more accurate data from the high-resolution geoclimatic factor map for Canada [14], suggested that the worldwide contour maps do not adequately take the effects of terrain into account. Indeed, it is known that the radiosonde data used to prepare the worldwide maps [15] were nonexistent or very sparse in such regions. From a comparison of predictions based on the worldwide and Canadian maps, a 6-dB decrease in the logarithmic geoclimatic factor  $G$  (or in the coefficient  $C_o$ ) was introduced for mountainous regions. This value also compared favorably with the 6- and 5-dB correction factors inherent in the methods of Morita [3] and Barnett [4], respectively.

*“Correction Factors” for Overwater Paths:* When the original model for  $K$  was adopted, few overwater data were available in the CCIR data base. The +5 dB correction factor in the logarithmic geoclimatic factor  $G$  (or in the coefficient  $C_o$ ) was based solely on data for links across the Strait of Georgia on the west coast of Canada, data for a link across the Bay of Fundy on the east coast, and knowledge that the 6-dB correction factors in the methods of Barnett [5] and Morita [6] were similar in magnitude (see [14] for data).

The bases for the revisions to this worldwide geoclimatic factor model are discussed in Section V.

#### IV. TESTS ON ITU-R PREDICTION METHODS FOR THE DEEP-FADING RANGE

##### A. The Worst-Month Fading Data Base

The ITU-R worst-month data base for the large fade-depth tail [18], [27] was employed for the tests. In all, data for 246 links in 23 countries were available (212 links over land and

TABLE III  
DISTRIBUTIONS AND EXTREME VALUES OF THE FOUR LINK PREDICTOR VARIABLES IN THE ITU-R DATA BASE (246 OVER LAND AND OVER WATER LINKS)

Predictor Variable	Minimum	5 %	10%	50%	90%	95%	Maximum
$d$ (km)	7.5	16.0	29.0	54.0	110.5	125.0	299.9
$f$ (GHz)	0.45	1.45	2.05	6.15	11.45	16.5	37.0
$l\epsilon_p$ (mrad)	0.0	0.12	0.3	1.94	11.0	15.5	36.5
$\phi$ (mrad)	0.0	0.9	1.7	4.5	15.7	19.8	41.3

34 over water) with values for at least the link variables of path length, frequency, and path inclination needed to test Method 1. Data for 239 links (206 over land and 33 over water) were available also with the value of the additional variable  $\phi$  needed to test Method 2; the only country for which path profiles are not yet available is Egypt. (The few values of  $\phi$  between zero and one were replaced by one to avoid negative values of  $\log \phi$ .) A map showing the geographical distribution of data is given in Fig. 2. Table III summarizes the distributions and extrema of the predictor variable values in the data base. More detailed information (including path profiles) is given elsewhere [27].

The amount and quality of the worst-month tail data is somewhat variable. For many of the links (141) data for 12 calendar months were available so that the statistics for the average worst month are in most cases very accurate. For a further large group of links (71), data for enough of the warmer calendar months are available to identify the worst-month statistics with a high degree of certainty. Finally, there are a small number of links (34) for which tail data were only available for one or a few months. These data were used in cases where the worst calendar month available was believed to be a worst month or close to a worst month, and where enough better data were not available for the country or region in question.

Among the first two groups of worst-month data noted above are data obtained during one year, and in some cases data obtained during two or more years. This allowed average worst-month statistical estimates to be obtained for individual links. Following the standard definition for average worst-

month statistics [25], in most cases the yearly worst-month percentages of time for which a given fade depth was exceeded were averaged over the number of years of data available. (It should be noted that in the definitive ITU-R recommendation on such statistics [25], the word "average" has been dropped in favor of the term "worst-month statistics," but an average is still implied. It should be noted also that the average worst-month statistics referred to are really average worst-calendar-month statistics, whereas the ITU-R definition in principle allows the month-long periods involved to begin at any day of a calendar month. However, the use of worst-calendar-month statistics is the only practical solution given the current ITU-R data base and the actual difference with true worst-month statistics is considered negligible in any case.) Of course, the worst calendar month for which this fade depth is exceeded can in principle be different for every year of data. However, in the case of a seven-link subset (the U.K. Mendlesham links [28]) of the 50 links with multiyear data, only average worst-calendar-month statistics were available rather than average worst-month statistics. Although such average worst-calendar-month percentages are expected to be smaller than true average worst-month percentages, the actual difference should be fairly small. This supposition was tested on the 116-km St. Chrischona-Jungfrau path in or around Switzerland, for which are available up to eight years of data at three frequencies [27]. Over the three frequencies, it was found that average-worst-month exceedances were only 48% larger than average worst-calendar-month exceedances. This corresponds to only a 1.7-dB difference in fade depth at a fixed percentage of time, which is smaller than the estimated contribution to the standard deviation in error due to year-to-year variability (see Section V-F).

In a small subgroup of the multiyear data base (about 9–15 links, seven of which are in one country—Finland), only data for the worst month in the entire measurement period were available. It was considered better to include these than not because of the shortage of data for the regions involved, and because there were only two years of data in most cases anyway. For these regions (e.g., Finland), apparent underpredictions of fading may be somewhat exaggerated.

In order to maximize consistency, the tail-point data for most links were obtained by the authors directly from cumulative distributions of fading provided, or acquired from the open literature. For the Italian data base, however, the available data [29] were in the form of a single probability occurrence factor obtained from a regression on the entire deep-fading portion of the cumulative distribution, which results in an equal weighing of the deep and shallow ranges despite the fact that the latter is more accurate. Because of the importance of these data in terms of quantity and coverage of a large range of climates and terrain, they were nevertheless included for testing purposes. Indeed, the standard deviations of error for Italy noted later in this section and in Section V are not much larger than those for countries for which more complete cumulative distributions were available.

Most of the data in the ITU-R data base were obtained by contacting officials of national or provincial telecommunications agencies in countries known to have significant data.

Some of these organizations were already participants of the then CCIR Study Group 5. Some data were made available in CCIR documents, or informally by administrations, once it became known that the CCIR was constructing a data base for testing purposes. Finally, a small group of data were obtained from the open literature in order to increase the amount available from tropical regions or other regions for which available data were sparse. Although some data without associated detailed path profiles were accepted in order to increase climatic coverage, 93.5% of the links do have path profiles (reproduced elsewhere [27]).

Notably missing from the ITU-R data base are data for the U.S. and Japan, both countries with private telecommunications networks and known prediction procedures (e.g., [3]–[5], [30]). The data available for Japan [3], although valuable for historical reasons, were not employed for testing purposes because the processing techniques used were not compatible with those from more recent data bases. Some data from these countries available in the open literature could be employed in the future in lieu of more complete data bases from private carriers. In any case, the current ITU-R data bank is one of the largest propagation data bases in existence and covers a wide range of climatic regions of the world.

### B. General Testing Procedures

As in previous analyses [2], [24] each data point was given equal weight regardless of whether the average worst-month statistics were based on one or more years of data. This procedure was considered appropriate since it is known that the effect of year-to-year variability on the overall error variance is considerably smaller than the inability of the prediction methods to fully describe the variability in link geometry and geoclimatic conditions (see Section V-F).

The error calculations were carried out by comparing predicted and measured fade depths (i.e., error = predicted fade depth minus measured fade depth) at the tabulated exceedance percentages in the large fade depth tail of the distributions. Since the distributions all have the same 10 dB/decade slope in principle (and statistically in practice [2]), this approach is equivalent to performing the calculations at a fixed fade depth such as the value  $A_{0.01}$  exceeded for 0.01% of the time.

### C. Testing Results for Observed Geoclimatic Factors

Table IV presents results for Methods 1 and 2 for countries and regions within these countries based on the use of observed geoclimatic factors as recommended by the CCIR [20]. Specifically it presents the observed mean logarithmic geoclimatic factors  $G$  for each region and the estimated standard deviation of the resulting prediction error obtained by calculating the values of  $G$  for each link from (3) and (6) using the observed values of  $A$  and  $p$ , and then averaging the values for the links in each region. Although it is recommended that Method 2 normally be used to obtain these factors [19], [20], Methods 1 and 2 were employed separately for the comparison in Table IV. Results for both overland and overwater links are given in Table IV. The number of links involved in the

TABLE IV  
MEAN OBSERVED LOGARITHMIC GEOCLIMATIC FACTORS AND STANDARD DEVIATIONS OF ERROR FOR  
ITU-R METHODS 1 AND 2 IN VARIOUS COUNTRIES AND REGIONS (AMERICAS, AFRICA, AND EUROPE)

Country (No. of links) Region	Mean $G$ (dB)	Sd. Dev. of Error (dB)
<b>Brazil</b>		
Curitiba Area Mts. (7)	2.8 (5.3)	5.5 (5.9)
<b>Canada</b>		
Ottawa Area (10)	5.1 (3.7)	3.7 (4.4)
Pr. George Area Mts. (5)	-9.6 (-7.7)	2.9 (2.4)
Creston Area Mts. (3)	-7.5 (0.8)	5.5 (3.4)
Vis. Melville Sound (4)	18.2 (14.3)	9.7 (8.0)

Country (No. of links) Region	Mean $G$ (dB)	Sd. Dev. of Error (dB)
<b>Egypt</b>		
Inland Nile Delta (3)	17.1	4.7
Coast/Oversea (2/1)	24.6	5.8
<b>Ghana</b> (3)	16.7 (15.5)	5.0 (3.4)
<b>Senegal</b> (3)	24.1 (22.9)	4.4 (3.7)
<b>Zimb./Moz./Mal.</b> (3)	-2.0 (2.0)	3.5 (3.8)

Country (No. of links) Region	Mean $G$ (dB)	Sd. Dev. of Error (dB)
<b>Finland</b>		
Gulf of Bothnia Coast (9)	12.1 (8.7)	4.7 (5.2)
<b>France</b>		
Brittany (5)	11.1 (10.0)	3.9 (4.0)
North East/Swi. (22)	6.5 (7.6)	4.9 (4.7)
South (9)	15.0 (15.6)	4.6 (5.4)
<b>Italy</b>		
North West Plain (9)	8.4 (8.0)	4.3 (5.8)
North East Plain (4)	18.8 (17.2)	4.2 (5.6)
North East Mts. (4)	-2.8 (2.3)	3.7 (2.7)
West Central (7)	8.9 (12.9)	5.7 (4.2)
Central Mts. (6)	4.7 (11.1)	3.0 (1.8)
N. West Oversea (7)	14.1 (18.8)	5.3 (8.1)
Sardinia Oversea (5)	5.8 (1.4)	5.7 (4.3)
<b>Norway/Denmark</b>		
S. Norway/Denmark (10)	7.1 (9.0)	4.8 (5.4)
Mid-North Oversea (3)	-1.9 (0.1)	5.5 (5.2)
<b>Sweden</b> (7)		
14.7 (14.4)	2.7 (3.9)	
<b>Switzerland</b> (15)		
3.7 (7.4)	3.9 (4.0)	
Alps Mts. (9)	3.6 (8.5)	4.2 (3.8)
<b>UK</b>		
East Anglia (8)	15.0 (15.2)	2.7 (2.5)
South West (4)	2.3 (5.4)	6.0 (6.0)
South/Midlands (8)	5.4 (2.9)	3.3 (2.0)
North East (8)	3.8 (3.3)	3.7 (3.5)
English Channel (3)	15.1 (14.8)	1.6 (0.9)
<b>Former USSR</b>		
Baltic Coast (6)	7.4 (3.3)	4.8 (4.2)
Byelorussia/Ukrn. (4)	5.3 (3.6)	4.0 (3.4)
Moscow Area (11)	5.7 (4.0)	5.9 (6.1)
Black Sea Coast (3)	9.1 (5.7)	0.1 (1.6)

TABLE V  
ERROR STATISTICS FOR ITU-R METHODS 1 AND 2 USING OBSERVED  
GEOCLIMATIC FACTORS FOR VARIOUS TERRAIN-CLIMATE LINK GROUPINGS

Link Grouping	No. of Links	Method 1		Method 2	
		Sd. Dev. of Error (dB)	% Errors > 7 dB	Sd. Dev. of Error (dB)	% Errors > 7 dB
Inland non- mountainous	90	4.4	11.1	4.5	11.1
Mountainous	29	3.8	6.9	3.6	3.5
Coastal	44	3.8	2.3	4.0	9.1
Overwater	21	5.6	19.1	6.3	33.3
All overland	187	4.1	8.6	4.2	8.6
All	210	4.3	9.5	4.4	11.0

calculations is indicated in parentheses after the country or region name. This approach yields overall mean errors of zero.

Regions were chosen on the basis of proximity of each link in geographic location and altitudes of the lower of the transmitting and receiving antennas. A similar approach was employed to develop the basic prediction formulas for Methods 1 and 2 [2]. Some of the larger standard deviations in Table IV are likely due to too large a range in geographical and altitude proximity. Some of the larger and smaller values may be due to too few data points within some regions. (Although a minimum of four links was sought for each region, in the case of countries with few data, this criterion was reduced to three.) The largest values tend to be those for overwater regions (see below). The exact attribution of links to each region is described elsewhere [27].

Error statistics by ITU-R terrain-climatic (i.e., "geoclimatic") type (including overall error statistics for overland

links and for overland/overwater links combined) based on the observed geoclimatic factors are presented in Table V. These statistics include the percentage of errors greater than 7 dB, a statistic giving a quantitative measure of the frequency of large errors. In order to provide a comparison of results for Methods 1 and 2, a common 210-link data base is employed. Overwater-link statistics are indicated, but excluding the results for five long links between the Italian mainland and Sardinia (all longer than 237 km) since it is considered that the current basic tail models are not accurate for very long links. (The maximum path length in the 47-link data base used to derive these relations was 95 km [2]; see also Section D below.) The same approach is taken for the overall statistics for both overland and overwater paths.

As indicated in Table V, the overall standard deviations of error for the common data base of 187 overland links are 4.1 dB for Method 1 and 4.2 dB for Method 2. These are larger than the 3.4 dB and 2.9 dB figures involved in the original fits for Methods 1 and 2 [2], but reasonable considering the greater diversity of link geometries now in the data base, the greater proportion of links with only one year of worst-month data and the use of a few groupings of only three links. Table V confirms the observation noted with respect to Table IV and elsewhere [14] that prediction accuracy is poorest for overwater links.

Fig. 3 gives distributions of the errors for Methods 1 and 2 on a normal probability plot. From these results and those of Tables IV and V, it is clear that the improvement of Method 2 over Method 1 observed with the original 47-link data base for the France and the U.K. [2] is not maintained in the

TABLE VI

ERROR STATISTICS FOR ITU-R ORIGINAL AND REVISED GEOCLIMATIC FACTOR MODELS FOR COUNTRIES\* AND REGIONS (AMERICAS, AFRICA, AND EUROPE)

Country (No. links) Region	Original Model		Revised Model	
	Mean Error (dB)	Sd. Dev. of Error (dB)	Mean Error (dB)	Sd. Dev. of Error (dB)
<b>Brazil (8)</b>	2.6 (0.5)	5.9 (6.3)	-0.4 (-2.5)	5.9 (6.3)
<i>Curitiba Area Mts. (7)</i>	2.2 (-0.3)	6.3 (6.3)	-0.8 (-3.3)	6.3 (6.3)
<b>Canada (21)</b>	4.3 (3.0)	6.1 (4.4)	1.5 (0.2)	6.3 (4.7)
<i>Ottawa Area (10)</i>	0.6 (2.1)	3.7 (4.4)	-2.4 (-0.9)	3.7 (4.4)
<i>Pr. George Mts. (5)</i>	9.4 (7.5)	2.9 (2.4)	7.4 (5.5)	3.0 (2.5)
<i>Creston Area Mts. (3)</i>	7.6 (-0.7)	5.5 (3.4)	4.6 (-3.7)	5.5 (3.4)
<b>Hudson Str/Frob. B (4)</b>	-1.4 (-0.5)	6.1 (7.0)	5.6 (6.5)	4.7 (5.7)
<i>Vis. Melville Sound (4)</i>	-8.4 (-4.5)	9.6 (7.9)	-7.9 (-4.0)	9.9 (8.2)

Country (No. links) Region	Original Model		Revised Model	
	Mean Error (dB)	Sd. Dev. of Error (dB)	Mean Error (dB)	Sd. Dev. of Error (dB)
<b>Egypt (6)</b>	-9.4	8.4	-1.4	8.4
<i>Inland Nile Delta (3)</i>	-6.9	4.8	-3.9	4.8
<i>Coast/Oversea (2/1)</i>	-13.5	9.1	-2.2	6.8
<b>Ghana (3)</b>	-2.5 (-1.4)	5.0 (3.4)	10.5 (11.6)	5.0 (3.4)
<b>Senegal (3)</b>	-4.3 (-3.2)	3.7 (3.7)	-1.3 (-0.2)	4.4 (3.7)
<b>Zimb./Moz./Mal. (3)</b>	8.3 (4.3)	4.2 (6.3)	11.3 (7.3)	4.2 (6.3)

\*Country error statistics (and no. of links) do not include overwater links

Error statistics for overwater regions in italics

Method 1 error statistics: No Parentheses  
 Method 2 error statistics: (Parentheses)

Country (No. links) Region	Original Model		Revised Model	
	Mean Error (dB)	Sd. Dev. of Error (dB)	Mean Error (dB)	Sd. Dev. of Error (dB)
<b>Finland (12)</b>	-21.8	4.8 (5.6)	-5.8 (-2.3)	4.3 (5.1)
<i>Gulf of Bothnia Coast (9)</i>	-22.2 (-18.3)	5.0 (5.5)	-6.0 (-2.6)	4.6 (5.0)
<b>France (30)</b>	-2.9 (-3.3)	4.8 (5.3)	0.9 (0.5)	5.0 (5.8)
<i>Brittany (5)</i>	-2.7 (-1.6)	4.0 (4.2)	2.4 (3.5)	3.2 (3.2)
<i>North East/Swi. (22)</i>	-2.7 (-3.8)	4.8 (5.2)	1.9 (0.8)	5.3 (5.4)
<i>South (9)</i>	-3.9 (-4.5)	4.4 (5.7)	0.7 (0.1)	5.7 (7.3)
<b>Italy (37)</b>	-1.4 (-4.1)	5.8 (6.3)	2.6 (-0.1)	6.3 (6.8)
<i>North West Plain (9)</i>	0.1 (0.5)	4.2 (5.7)	3.1 (3.5)	4.2 (5.7)
<i>North East Plain (4)</i>	-11.3 (-9.6)	4.0 (5.5)	-6.3 (-4.7)	7.8 (9.1)
<i>North East Mts. (4)</i>	7.4 (2.4)	1.2 (1.5)	10.4 (5.4)	1.2 (1.5)
<i>West Central (7)</i>	-4.1 (-8.1)	3.4 (3.5)	-0.2 (-4.2)	5.6 (5.5)
<i>Central Mts. (6)</i>	-0.6 (-7.0)	1.5 (2.6)	2.4 (-4.0)	1.5 (2.6)
<i>N. West Oversea (7)</i>	-0.1 (-4.8)	5.3 (8.2)	7.9 (3.2)	5.3 (8.2)
<i>Sardinia Oversea (5)</i>	8.5 (12.9)	5.8 (4.4)	16.5 (20.9)	5.8 (4.4)
<b>Norway/Denmk (11)</b>	-8.6 (-10.7)	6.9 (6.6)	2.1 (0.0)	6.8 (7.0)
<i>S. Norway/Denmk (10)</i>	-10.1 (-12.0)	5.1 (5.4)	0.7 (-1.2)	5.3 (6.1)
<i>Mid-North Oversea (3)</i>	3.7 (1.8)	5.8 (5.5)	18.7 (16.8)	5.8 (5.5)
<b>Sweden (7)</b>	-21.5 (-21.3)	2.8 (4.1)	-4.7 (-4.5)	4.7 (4.4)
<b>Switzerland (15)</b>	-3.4 (-7.2)	4.1 (4.2)	2.0 (-1.8)	5.1 (6.0)
<i>Alps Mts. (9)</i>	-3.4 (-8.3)	4.6 (3.9)	-0.4 (-5.3)	4.6 (3.9)
<b>UK (28)</b>	-6.0 (-5.6)	7.2 (7.1)	1.7 (1.6)	5.7 (5.0)
<i>East Anglia (8)</i>	-14.9 (-15.1)	2.6 (2.4)	-2.5 (-2.7)	2.9 (2.4)
<i>South West (4)</i>	2.2 (-0.9)	6.8 (6.7)	7.6 (4.5)	8.5 (8.2)
<i>South/Midlands (8)</i>	-2.8 (-0.3)	4.0 (2.9)	0.9 (3.4)	4.9 (3.9)
<i>North East (8)</i>	-4.3 (-3.8)	3.7 (3.4)	2.0 (2.5)	4.7 (4.2)
<i>English Channel (3)</i>	-8.6 (-8.3)	1.6 (0.9)	-0.6 (-0.3)	1.6 (0.9)
<b>Former USSR (27)</b>	-6.1 (-4.0)	7.1 (6.6)	0.7 (2.7)	5.9 (6.0)
<i>Baltic Coast (6)</i>	-12.4 (-8.3)	5.2 (4.7)	0.9 (4.9)	3.2 (1.8)
<i>Byelorussia/Ukrn. (4)</i>	-5.3 (-3.7)	6.7 (5.9)	-2.3 (-0.7)	6.7 (5.9)
<i>Moscow Area (11)</i>	-7.2 (-5.5)	6.4 (6.6)	-1.4 (0.2)	5.8 (6.0)
<i>Black Sea Coast (3)</i>	1.8 (5.1)	0.6 (2.1)	8.1 (11.5)	5.8 (4.9)

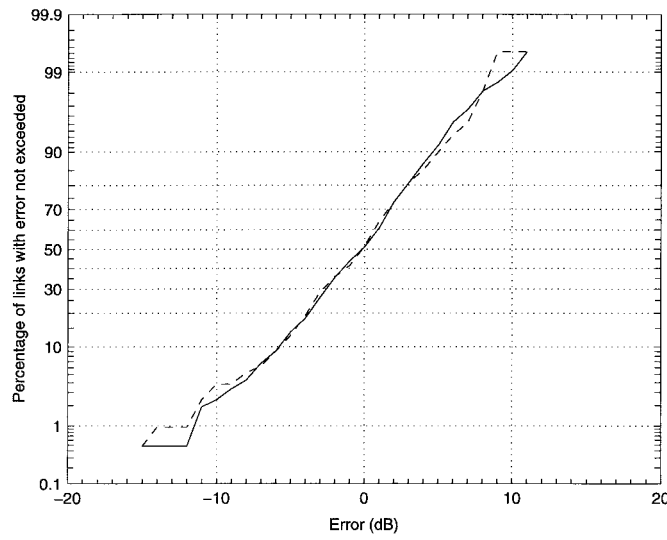


Fig. 3. Distributions of errors for all 210 links (including overland and overwater) using observed mean geoclimatic factors in various regions (at least three links per region): — Method 1; - - - Method 2.

enlarged data base; in fact, for coastal and overwater links it is significantly worse. Thus, there would seem to be no advantage to be gained in using Method 2 in its present form, at least when observed  $G$  values are available. However, as noted in Section V-F, new regressions on the same three and four variables used for Methods 1 and 2, employing the enlarged

187-link overland data base, demonstrate a small advantage to using the additional variable.

#### D. Testing Results for Predicted Geoclimatic Factors

Table VI presents the error statistics for countries and regions based on both the original and revised geoclimatic factor models. Since the mean errors are no longer zero, these are also presented along with the standard deviations of error.

Error statistics by terrain-climatic type, based on predicted geoclimatic factors, are presented in Tables VII and VIII for the original and revised geoclimatic factor models, respectively. Here, the percentage of errors greater than 10 dB from the mean error is also given, as a measure of the frequency of large errors. Further, the standard deviations of mean error from region to region are also presented, with each mean error properly weighted according to the number of links in the region (which allows even single-link regions to be included in the calculation). Shown are the combined Method 1 statistics using the entire 240-link data base (in square brackets), and those for the common 233-link data for a comparison of Methods 1 and 2 (errors for the six overwater paths from the Italian mainland to Sardinia and Sicily longer than 237 km are not included for the reasons already noted). The number of mountainous links is smaller for the tests on the revised model since eight links for which the lowest terminal is below 700 m in altitude are excluded, even though the major portions of the links are over mountains.

TABLE VII

ERROR STATISTICS FOR METHODS 1\* AND 2 WITH CCIR ORIGINAL GEOCLIMATIC FACTOR MODEL FOR VARIOUS TERRAIN-CLIMATIC LINK GROUPINGS

Link Grouping	No. of Links	Method 1 (Original)				Method 2 (Original)			
		Overall Mean Error (dB)	Sd. Dev. of Reg. Mean Errors (dB)	Sd. Dev. of Error (dB)	% of Errors <Error> > 10 dB	Overall Mean Error (dB)	Sd. Dev. of Reg. Mean Errors (dB)	Sd. Dev. of Error (dB)	% of Errors <Error> > 10 dB
Inland non-mountainous	104 [107]	-3.1 [-3.2]	5.1 [5.1]	6.5 [6.5]	12.5 [11.2]	-2.9	5.0	6.6	13.5
Mountainous <sup>†</sup>	44	1.0	5.2	6.4	6.8	-3.6	5.6	6.7	9.1
Coastal <sup>†</sup>	58 [61]	-11.0 [-11.1]	9.1 [9.1]	9.7 [9.8]	37.7 [38.3]	-10.1	8.3	9.1	27.6
Overwater	27 [28]	-0.5 [-0.7]	5.7 [5.6]	7.7 [7.6]	18.5 [17.9]	-1.4	5.0	7.6	11.1
High lat. ( $\geq 60^\circ$ )	28	-11.9	10.6	11.7	39.3	-10.2	8.8	10.1	42.9
All overland	206 [212]	-4.4 [-4.6]	7.7 [7.8]	8.7 [8.7]	24.8 [24.5]	-5.1	6.8	8.0	20.4
All	233 [240]	-4.0 [4.1]	7.6 [7.7]	8.7 [8.7]	24.0 [23.8]	-4.6	6.7	8.1	21.5

\* Results in square brackets include data for the seven links in Egypt.

<sup>†</sup> Note that although the definition of mountainous links in the original method was somewhat vague, it could be implied that a link should be considered mountainous if at least half the path profile was over mountains. Here it was assumed that at least half the path profile was above 700 m in altitude. Since there were no links in the data base from the flat central plains of the continents (some of which are above 700 m; see section V.E), this is considered a reasonable assumption in comparison to the less restrictive criterion in the revised method for which results are given in Table VIII. Although there was no definition for coastal links in the original method, for comparison purposes results are presented here for the original method as applied to the same coastal grouping for which results are given for the revised method in Table VIII.

TABLE VIII

ERROR STATISTICS FOR METHODS 1\* AND 2 WITH ITU-R REVISED GEOCLIMATIC FACTOR MODEL FOR VARIOUS TERRAIN-CLIMATIC LINK GROUPINGS

Link Grouping	No. of Links	Method 1 (Revised)				Method 2 (Revised)			
		Overall Mean Error (dB)	Sd. Dev. of Reg. Mean Errors (dB)	Sd. Dev. of Error (dB)	% of Errors <Error> > 10 dB	Overall Mean Error (dB)	Sd. Dev. of Reg. Mean Errors (dB)	Sd. Dev. of Error (dB)	% of Errors <Error> > 10 dB
Inland non-mountainous (100-400 m min. antenna altitude)	66 [67]	-0.6 [-0.6]	3.6 [3.6]	5.2 [5.2]	6.1 [6.0]	0.6 [0.6]	3.3 [3.3]	5.1 [5.0]	6.1 [6.0]
Inland non-mountainous (400-700 m min. antenna altitude)	24	5.0	3.6	4.4	0.0	1.6	3.9	4.8	4.2
Inland non-mountainous	111 [114]	0.4 [0.3]	3.8 [3.8]	5.7 [5.7]	11.4 [11.3]	0.4	3.4	5.5	8.1
Mountainous (700-1000 m min. antenna altitude)	18	1.9	4.7	5.7	11.1	-3.4	4.7	5.3	5.6
Mountainous (1000-1300 m min. antenna altitude)	15	2.9	6.2	7.1	13.3	-0.9	7.7	6.6	6.7
Mountainous	37	2.8	4.9	6.2	8.1	-2.2	5.2	6.3	8.1
Coastal (medium-sized)	10	-0.6	3.3	5.8	0.0	1.9	4.1	6.3	20.0
Coastal (large)	38 [41]	3.5 [3.3]	5.9 [6.2]	6.6 [6.9]	7.9 [12.2]	3.3	5.9	6.8	10.5
Coastal	57 [61]	1.3 [1.3]	6.1 [6.2]	7.0 [7.2]	13.8 [16.4]	2.3	5.5	6.7	15.5
Overwater (medium-sized)	6	7.3	4.9	5.4	0.0	5.6	5.1	6.0	0.0
Overwater (large) <sup>†</sup>	21 {27} [22]	5.3 {7.6} [5.3]	8.7 {8.8} [8.5]	10.3 {10.3} [10.1]	28.6 {37.0} [27.3]	4.7 {7.9} [10.1]	7.4 {9.1} [27.3]	9.7 {10.8} [27.3]	28.6 {33.3}
Overwater <sup>†</sup>	27 {33} [28]	5.8 {7.6} [5.7]	7.9 {8.2} [7.8]	9.4 {9.6} [9.2]	25.9 {30.3} [25.0]	4.9 {7.5} [25.0]	6.9 {8.5} [10.0]	8.9 {10.0} [27.3]	22.2 {27.3}
High lat. ( $\geq 60^\circ$ )	28	-0.5	6.0	10.5	32.1	1.1	7.4	8.7	28.6
All overland	206 [212]	1.1 [1.0]	4.4 [4.5]	6.2 [6.3]	12.1 [12.7]	0.5	4.2	6.2	9.7
All	233 [240]	1.6 [1.6]	5.1 [5.2]	6.8 [6.8]	14.2 [14.6]	1.0	4.8	6.7	12.9

\* Results in square brackets [ ] include data for additional links in Egypt.

† Results in curly brackets { } include data for six links longer than 237 km in Italy, but not additional link in Egypt.

From Table VII, the overall mean and standard deviations of error for the original model for the 206 overland links are, respectively,  $-4.4$  dB and 8.7 dB for Method 1, and  $-5.1$  dB and 8.0 dB for Method 2. The large negative mean errors are mainly due to the large negative errors for high-latitude links and the preponderance of European links with negative mean errors in the data base. The large standard deviations are due to the large variation in the mean errors between countries. Without the mean error variations between countries, the overall standard deviation would be 6.2 and 6.1 dB for Methods 1 and 2, respectively.

## V. DISCUSSION OF RESULTS AND BASIS FOR THE REVISED GEOCLIMATIC FACTOR MODEL

Although the standard deviations of error listed in Table VI for the original geoclimatic factor model applied to individual

countries or regions are acceptable, the mean errors and the resulting large overall standard deviation of error are not. Since analysis showed that the errors resulting from the geoclimatic factor model are the largest contributors (see Section F below), several improvements were made to achieve the considerably better error statistics for the revised model listed in Tables VI and VIII.

### A. Development of the Continental Longitude Correction Factor

The apparent need for a longitude correction to the original geoclimatic factor models for Methods 1 and 2 is illustrated in Table VI by the preponderance of negative mean errors for mid- and low-latitude countries in Europe (e.g., France, Italy, Switzerland, U.K., and the former USSR) and Africa (Egypt, Ghana, Senegal) and the positive mean errors for the Americas

(Brazil and Canada). Although a longitude difference was recognized during the development of the original geoclimatic factor model, there were insufficient data then to justify a more complex model. The mean error between the European and North American groups of data available then was set approximately to zero.

The need for a longitude correction is believed to be due to the fact that the maps from which the statistic  $p_L$  is derived are based on only two radiosonde ascents per day that take place at the same time (0 and 1200 UT) around the world. Since the atmospheric conditions that give rise to multipath fading (i.e., extreme superrefractive refractivity gradients) are quite dependent on local time, the change in the radiosonde sampling time relative to these conditions produces different results for large longitude differences.

The discrete continental longitude correction factors of (17) to (19) were derived by calculating the mean errors for two groups of data [31]: overland data for nonmountainous noncoastal mid- or low-latitude regions in Brazil and Canada for the Americas; and in France, Italy, the U.K., the former USSR, Egypt, Ghana, and Senegal for Europe/Africa. Data from mountainous, coastal, and high-latitude regions were not used in order to avoid contamination from the other climatic effects on the geoclimatic factor.

In the future, it may be possible to derive a suitable correction factor that is continuously variable with longitude. Although some research has already been carried out in this direction, it may be better to couple such research with new regression analyses on the link variables using the much larger data base now available. Better still, a climatic variable based on surface measurements carried out several times a day may be found that obviates the need for a correction factor.

### B. Development of the High-Latitude Correction Factor

The need for a high-latitude correction to the original geoclimatic factor model is best illustrated by the large negative mean errors in Table VI for Finland, Norway/Denmark, Sweden, and the Baltic coast region of the former USSR. It is also illustrated by the Canadian data [14], but because these data are for overwater paths, the interpretation is more difficult.

This need is again believed due to the limitation of only two radiosonde ascents per day in sampling the refractive structure of the atmosphere. Two sets of data, one for overwater paths in the Hudson Strait area [32] and the other for very-low-angle satellite links [33], indicate clearly that multipath fading at high latitudes tends to take place at all hours of night and day, regardless of the fact that the day is longer in summer. Although  $p_L$  statistics can be used for prediction purposes, a different fit is, in effect, required.

The correction factor of 7 dB for latitudes above  $60^\circ$  in (16) was developed from the data for Finland, Norway/Denmark, Sweden, and the Baltic coast region of the former USSR [31]. A 5 dB factor had previously been used for Canada [14], but since the refractivity gradient statistic  $p_d$  employed to develop the basic geoclimatic factor map is not identical to  $p_L$ , it is not clear that the high-latitude correction factors should be identical. Since the Canadian high-latitude links were all over

water, the accuracy of the 5-dB figure was somewhat suspect in any case. Since much of the Finnish and Swedish data had the additional complication of being from coastal regions, the Norwegian/Danish data were principally used to determine the 7-dB figure above  $60^\circ$  [31]. The extensive data for the Moscow region were used to determine the rate of decrease with decreasing latitude of (15). However, at the time this was done, the Method 2 results for this region were unavailable [31].

An iterative approach to the choice of the high-latitude correction factor and the overwater/coastal correction factors (see below) could result in slightly more accurate values for each. However, as for the continental longitude correction factor, discovery of a better climatic variable based on surface measurements carried out several times a day could eliminate the need for a high-latitude correction factor.

### C. Improvement of the Overwater Correction Factor

As indicated in Table I, the geoclimatic correction factor in the original model for overwater links was 5 dB. Two new factors were established in the revision, a 6-dB correction for links over "medium-sized" bodies of water and a 10 dB correction for links over "large" bodies of water. The 6-dB factor was principally determined [31] by the data for the Bay of Fundy and Strait of Georgia [14], data for Morecomb Bay in the Irish Sea [27], and data for two links in Frobisher Bay [14]. The 10-dB factor was principally determined from the data for the English Channel [27] in combination with the data for Hudson Strait and Viscount Melville Sound [14], [27]. (Coastal data for East Anglia in the U.K. and parts of Scandinavia were also considered; see below.) The 14-dB factor used originally for large bodies of water [14] was revised by giving the European overwater data more weight in the more recent analysis, because it was uncontaminated by high-latitude effects. The greatest weight was given to overwater data (e.g., the English Channel) for which there were also extensive nearby overland data.

The overall mean errors for overwater links in Table VIII would suggest that the revised overwater correction factors are much too large. A new analysis [34], however, indicates the prediction problem to be more complex than this. It was found that predictions for both overwater and coastal links are improved by using a separate, considerably smaller, climatic dependence to that used for inland links. It was also found that climatic variability for overwater and coastal links could be better described by latitude than by the climatic predictor variable  $p_L$ . The end result is that the effective overwater/coastal correction factor appears to vary not only with the size of the body of water in question, but also with latitude. In general, it appears to be small at low latitudes, and increases with increasing latitude. In fact, the overwater correction factors developed initially from high-latitude data [14] and mid-latitude data [31] are not inconsistent with the results from the new overwater/coastal model [34] in these areas.

Table VI suggests that the overwater predictions for the links between the mainland of Italy and Sardinia are inac-

curate. A similar result was obtained for the single overwater link between the mainland and Sicily. This is believed to be largely due to the extreme length of these links (237–300 km) for which the power law in path length in the models is inappropriate. Initial results suggest that a new regression on the available data will provide a much better fit for such long links. The results of Tables VII and VIII in most cases do not include these links. However, results for the overwater group in Table VIII are provided with and without these links.

#### D. Development of the Coastal Correction Factor

The need for some kind of coastal correction is best illustrated by the negative mean errors for the original model in Table VI for East Anglia in the U.K., the northeast plain of Italy near Bologna and Venice, the Baltic coast region of the former USSR, and the Mediterranean coastal area of Egypt. Since the factors required seemed to be approximately equivalent to the overwater correction factors for the nearby bodies of water in question, this is what was adopted in the revised model [31].

The criteria adopted by the ITU-R [19] for determining a coastal area in the revised geoclimatic factor model (Note 2 below Table II) are essentially identical to those employed for the CCIR/ITU-R transhorizon duct propagation model [35]. From an observation of the data for various regions of the U.K. and Brittany in France and the accurate path profiles available [31], they appeared to be valid for the line-of-sight (LOS) geometry as well. The procedure for determining the magnitude of the correction in cases where part of a path profile is above 100-m altitude is also similar.

The data for Finland [27] suggested the need for a similar correction factor for regions of many lakes (see Note 3 below Table II). Unfortunately, a precise criterion for providing such a factor is impossible without additional data.

It should be noted that nine links were classified as lying in coastal regions beside bodies of water of intermediate size and were given a correction factor of 8 dB. These are not included in the error statistics for either coastal links beside medium-sized or large bodies of water. The choice of whether a body of water was considered medium-sized or large (or intermediate between these two) was made prior to the error calculations, except in the case of the few links on which the 6- and 10-dB figures (and the respective examples of medium-sized and large bodies of water in Table II) were based.

As noted above and demonstrated for Method 1 elsewhere [34], predictions for coastal/overwater links are improved even more by decoupling them from predictions for hypothetical inland links at the same location, and employing a different climatic dependence to that for inland links.

#### E. Improvement of the Mountain Correction Factor

The original correction factor of –6 dB for links in mountainous regions has been clarified [31] with the 700-m minimum altitude limit now specified in the revised model [19]. The altitude of the lower of the transmitting and receiving antennas (termed here the “minimum altitude”) was found to be a good variable from which to assess mountainous behavior

for the links in the ITU-R data base (see below regarding links over high-plains regions). Several links in both Italy and Switzerland with quite high-altitude antennas at one end of the path (and a large fraction of the path over mountains), but low-altitude antennas at the other, were found to have similar observed geoclimatic factors to those of nearby links with low antennas at both ends. In fact, it was found possible to group all the links in northeastern France with six of those in Switzerland having one antenna of comparable altitude (see Table VI).

From the mean errors of Table VIII, the –6 dB mountain correction factor for both Methods 1 and 2 would be better replaced by factors of about –8.5 and –3.5 dB, respectively, in order to reproduce a slightly positive mean error such as obtained for inland links in nonmountainous regions. Not shown, this has been confirmed. (It must be noted, however, that although the –8.5 and –3.5 dB factors are better on average, there are some mountainous regions—possibly in which the altitude and/or geographical extent of the mountains is smaller as apparently evidenced from Table VI—in which a less negative factor seems more appropriate.)

From the mean errors for the 100–400- and 400–700-m minimum altitude ranges, it is evident that a better discrete correction would employ approximately –5 and –1.5 dB corrections for altitudes between 400 and 700 m for Methods 1 and 2, respectively. The smaller corrections required for Method 2 in medium and high-altitude ranges demonstrates another benefit of the additional predictor variable  $\phi$ . It is expected that a future terrain correction factor can be devised in which the correction is continuously variable depending on the minimum altitude predictor variable or a similar one such as the minimum altitude along the path and some measure of the terrain roughness. Indeed, an interim improvement to Method 1 has already been devised [36], [37] employing discrete corrections for the 100–400- and the 400–700-m altitude ranges along with corrections based on a subjective assessment of whether the link is in a plains region, a hilly region or a region of uncertainty between these two.

An oversight in the revision of the ITU-R methods was the lack of consideration of links in relatively flat plains regions or hilly regions for which the minimum antenna altitude is above 700 m. Although no data are available for such links in the current ITU-R data base, an estimate of the correction factor required for high-plains links [36], [37] was obtained from the high-resolution Canadian geoclimatic-factor map in [14, Fig. 3]. A conservative estimate of the correction factor required for high-altitude links in hilly regions [37] was then set relative to this based on the known 3.5-dB average geoclimatic difference [36] between links in plains and hilly regions at low altitude.

#### F. Effect of the Various Model Elements on the Overall Accuracy of the Methods

Because of the apparently small improvement afforded by Method 2 over Method 1 and the large reduction of error achieved by the revision to the geoclimatic factor model, it is useful to obtain a quantitative measure of the various pre-

dition errors. It seems reasonable that the overall variance of the fade depth prediction error (i.e., the square of the standard deviations given in Tables VI–VIII) can be represented as follows:

$$\sigma^2 = \sigma_y^2 + \sigma_v^2 + \sigma_G^2 \quad (21)$$

where  $\sigma_y^2$  is the variance due to year-to-year variability in the fade depth observed in the worst month (or in the case of links with more than one year of data, in the observed average worst-month fade depth over the number of years in question),  $\sigma_v^2$  is the variance in the error due to the regression fit in terms of the link variables and  $\sigma_G^2$  is the variance in the error due to the geoclimatic factor model. Since the number of worst months of data involved varies from link to link,  $\sigma_y^2$  is, of course, an average over the whole data base.

Some idea of the magnitude of  $\sigma_y$  can be obtained from links for which fading data [27] are available for several years. For example, an estimated single-year value of  $\sigma_y = 2.2$  dB was obtained from the 116 km, 2.3 GHz link between St. Chrischona and Jungfraujoch in Switzerland, for which eight years of worst-month data are available. An estimated single-year value of  $\sigma_y = 4.0$  dB was obtained from the 12.7 km, 19.3 GHz link near Dubna, Russia, for which eight years of data are available also. There are 16 overland links in the ITU-R data base for which there are three or more years of worst-month fade depths. An average of the  $\sigma_y^2$  estimates for all of these links yields an overall single-year estimate of  $\sigma_y = 2.5$  dB. (The central 75% of these values are in the range 1.0–3.1 dB. Except for an apparent inverse dependence on path length between the two eight-year examples above, there is no obvious dependence on link parameters.) The resulting figure for the data base for which on average there are 1.5 years of worst-month data, can be estimated from

$$\sigma_y = \sqrt{\frac{2.5^2}{n} \left[ \sum \frac{1}{N_i} \right]} = 2.3 \text{ dB} \quad (22)$$

where  $N_i$  is the number of years for which worst-month data are available for link  $i$  [27] and  $n$  is the total number of overland links (212 links for which results for both Methods 1 and 2 are available).

To a first approximation  $\sigma_G$  can be assumed to be zero for predictions using the observed regional average values for the geoclimatic factor. From the results of Table V for overland links

$$\sigma_v = \sqrt{4.1^2 - 2.3^2} = 3.4 \text{ dB} \quad \text{Method 1} \quad (23)$$

$$\sigma_v = \sqrt{4.2^2 - 2.3^2} = 3.5 \text{ dB} \quad \text{Method 2.} \quad (24)$$

More generally, there will be some residual value of  $\sigma_G$  even for the predictions using observed average geoclimatic factors. This is because there is some natural geoclimatic variation that cannot be avoided within zones of finite size and altitude range. Thus, the figures in (23) and (24) should be upper bounds.

The contribution of errors in the geoclimatic factor model can be readily determined by combining the error statistics of Tables V and VII. Thus, for the original geoclimatic factor

model

$$\sigma_G = \sqrt{8.7^2 - 4.1^2} = 7.7 \text{ dB} \quad \text{Method 1} \quad (25)$$

$$\sigma_G = \sqrt{8.1^2 - 4.2^2} = 6.9 \text{ dB} \quad \text{Method 2.} \quad (26)$$

Thus, by far the greatest contribution to the errors in Methods 1 and 2 with the original geoclimatic factor model is in the estimate of  $G$ .

For the revised geoclimatic factor model

$$\sigma_G = \sqrt{6.3^2 - 4.1^2} = 4.8 \text{ dB} \quad \text{Method 1} \quad (27)$$

$$\sigma_G = \sqrt{6.2^2 - 4.2^2} = 4.6 \text{ dB} \quad \text{Method 2.} \quad (28)$$

Clearly the revised geoclimatic factor model is considerably more accurate than the original model, which is the reason for the considerable reduction in the overall standard deviation of error. However,  $\sigma_G$  is still larger than  $\sigma_v$ . (In the new interim improvement to Method 1 [37],  $\sigma_G = 3.2$  dB for overland links, and 4.0 dB for all links.)

The results of (27) and (28) demonstrate that it is statistically better to estimate  $G$  in a region by the data from even a single link, since the standard deviations of error of the observed  $G$  values are 4.1 and 4.2 dB for Methods 1 and 2, respectively (i.e., the same as the standard deviations of error for estimating  $A$  from observed  $G$  values). Data for two links in a region will reduce the standard deviation of error in predicting  $G$  by  $1/\sqrt{2}$ , etc.

Strictly speaking,  $\sigma$  is only the apparent standard deviation of error. The actual standard deviation of error  $\sigma_a$  can be estimated from

$$\sigma_a = \sqrt{\sigma_v^2 + \sigma_G^2} \quad (29)$$

by removing the effect of year-to-year variability in the data. Thus, for all the overland data

$$\sigma_a = 5.9 \text{ dB} \quad \text{Method 1} \quad (30)$$

$$\sigma_a = 5.8 \text{ dB} \quad \text{Method 2.} \quad (31)$$

Clearly, the improvement afforded by Method 2 over Method 1 is very small in terms of all of the error statistics provided. This is further supported by the distribution of errors for each method in Fig. 4. Thus, it is now fully evident that there is no significant statistical advantage to be gained by employing Method 2 over Method 1 (at least in its present form), even though it contains an additional predictor variable.

It is known that  $\sigma_v$  can be reduced further by performing new regressions on the much enlarged data base now available. Indeed, a regression using the existing variables of Methods 1 and 2 on all the available overland data for regions with three or more links per region (187 links total) reduces the standard deviation of error for all overland links from 4.1 to 3.9 dB and from 4.2 to 3.7 dB, respectively, when observed mean  $G$  values are employed for the various regions. Thus, with new regressions, the small improvement in accuracy of the four-variable regression over the three-variable regression [2] is regained. On the basis of the earlier analysis [2] and more recent analyses, however, it is expected that even further improvement may be possible by introducing one or more new variables.

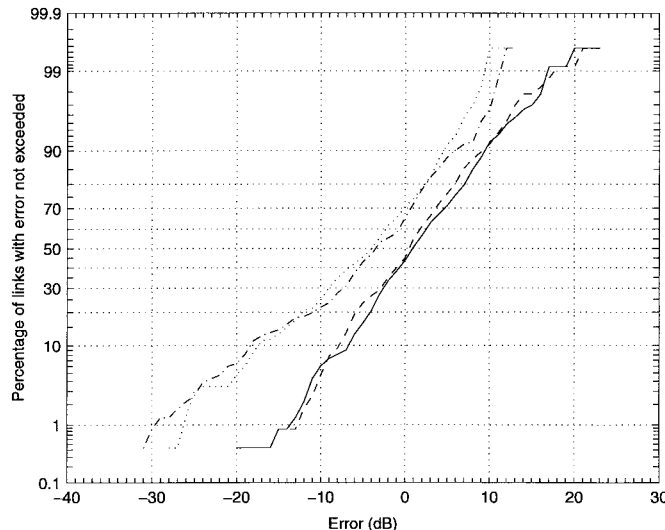


Fig. 4. Distributions of errors for all 233 links (including overland and overwater) using predicted geoclimatic factors: - - - Original Method 1; · · · · · Original Method 2; — Revised Method 1; - - - Revised Method 2.

For most or all of the improvement in  $\sigma_v$  of a multivariable model such as Method 2 to be translated into  $\sigma$  or  $\sigma_a$ , some means must also be sought to reduce  $\sigma_G$  significantly. Three main avenues of reducing  $\sigma_G$  are being pursued by the authors and others: one involves the introduction of more accurate maps for the climatic variable and possibly the use of a different climatic variable altogether [38], [39]. Another involves the introduction of one or more terrain variables (e.g., minimum antenna altitude) in addition to the climatic variable. Finally, the third involves regressions on all available observed geoclimatic factors to replace the “two-region” slope of (20).

## VI. SUMMARY AND CONCLUSIONS

This paper has provided the basis of the original (1988) and revised (1993) versions of ITU-R Methods 1 and 2 for predicting the deep-fading portion of the multipath fading distribution on terrestrial LOS links at various locations around the world in the average worst month, along with the results of the most extensive tests on these methods to date. The ITU-R data base assembled by the authors contained data for 246 links in some 23 countries at frequencies between 450 MHz and 37 GHz in regions from mountainous to over water. Detailed results were presented on the basis of countries, regions within countries, and terrain-climatic regions.

The error statistics demonstrate the considerable improvement of the revised geoclimatic factor model over the original model. The ability of the revised model to follow the large-scale climatic variability over a large area of the world is evidenced by the relatively small mean errors from country to country, and from region to region within countries. At the same time they demonstrate that no significant overall advantage is gained by employing Method 2 (with its additional variable obtained from a calculation on the path profile) over Method 1, at least in its present form. Overall mean and standard deviations of error for revised Methods 1 and 2 on overland paths are 1.0 and 6.2 dB and 0.4 and 6.1

dB, respectively. Nevertheless, the slightly better ability of Method 2 to follow large-scale geoclimatic variations from one region to another (4.1 versus 4.5 dB for the standard deviation of regional mean errors) suggests the possibility of future improvements using one or more path-profile predictor variables.

On the basis of a detailed analysis of the various sources of error, it was shown that the largest contribution to the overall standard deviation of error is that due to the geoclimatic factor model. The corresponding contribution to the overall standard deviation of error on overland paths was estimated as 4.8 dB for Method 1, whereas that due to the link-variable model (the next most important) was estimated to be at most 3.4 dB. Since these errors must be combined in terms of the corresponding variances, future work to improve the geoclimatic factor model is clearly important.

## ACKNOWLEDGMENT

The authors would like to thank L. Martin who provided the initial *raison d'être* for this work while the authors *d'être* were Guest Researchers at the Centre National d'Études des Télécommunications (CNET), Lannion, France from 1983 to 1985. They would also like to thank several colleagues who made an effort to provide unpublished data for testing purposes: M. Caskey, J. Doble, M. T. Hewitt, K. Hughes, R. Laine, M. Liniger, L. Martin, L. Nadenenko, L. Saini, P. Thorvaldsen, T. Tanem, D. Vergeres, and A. R. Webster. Many CCIR/ITU-R and other colleagues provided helpful discussions or contributions to other aspects of the work. The authors would particularly like to thank L. Martin and B. Segal. Finally, they would like to thank M. Hall for providing the initial vision for a formal CCIR testing process and a conducive atmosphere along the way.

## REFERENCES

- [1] A. Giger, *Low-Angle Microwave Propagation: Physics and Modeling*. London, U.K.: Artech House, 1991.
- [2] T. Tjelta, R. L. Olsen, and L. Martin, "Systematic development of new multivariable techniques for predicting the distribution of multipath fading on terrestrial microwave links," *IEEE Trans. Antennas Propagat.*, vol. 38, pp. 1650-1665, Oct. 1990.
- [3] K. Morita, "Prediction of Rayleigh fading occurrence probability of line-of-sight microwave links," *Rev. Elec. Comm. Lab. (Japan)*, vol. 18, pp. 310-321, Nov./Dec. 1970.
- [4] W. T. Barnett, "Multipath propagation at 4, 6, and 11 GHz," *Bell Syst. Tech. J.*, vol. 51, pp. 321-361, Feb. 1972.
- [5] A. Vigants, "Space diversity engineering," *Bell Syst. Tech. J.*, vol. 54, pp. 103-142, Jan. 1975.
- [6] K. W. Pearson, "Method for the prediction of the fading performance of a multisection microwave link," *Proc. Inst. Elect. Eng.*, vol. 112, pp. 1291-1300, July 1965.
- [7] J. E. Doble, "Prediction of multipath delays and frequency selective fading on digital radio links in the UK," *Inst. Elect. Eng. Dig.*, no. 62, 1979.
- [8] L. V. Nadenenko, "Kraschutu ustoychivosti signala na intervalakh radio releynih liniy pryamoy vidnosti (Calculation of signal stability in line-of-sight radio-relay systems)," in *Proc. NIIR*, 1980, vol. N5, (in Russian).
- [9] CCIR Rep. 338-6, "Propagation data and prediction methods required for terrestrial line-of-sight systems," in *XVIIth Plenary Assembly Int. Telecommun. Union—Rep. CCIR Annex vol. V*, Geneva, Switzerland, 1990, pp. 355-420.
- [10] L. Boithias, "Distribution statistique des niceaux reçus en propagation par trajets multiples troposphériques (Statistical distribution of received

levels in tropospheric propagation)," *Ann Télécommun.*, vol. 36, pp. 329–337, May/June 1981.

[11] ———, *Radio Wave Propagation*, English ed. New York: McGraw-Hill, 1987 (transl. D. Beeson).

[12] CCIR Rep. 338-5 (MOD I), "Propagation data and prediction methods required for line-of-sight radio-relay systems," in *Concl. Interim Meet. Study Group 5, Int. Telecommun. Union*, Geneva, Switzerland, July 1988, Doc. 5/204, pp. 166–233.

[13] CCIR Doc. 5/122 (Canada), "Prediction of the multipath fading distribution on terrestrial fixed line-of-sight links in the UHF and SHF bands," in *Int. Telecommun. Union*, Geneva, Switzerland, Mar. 1988.

[14] R. L. Olsen and B. Segal, "New techniques of predicting the multipath fading distribution on VHF/UHF/SHF terrestrial line-of-sight links in Canada," *Can. J. Electr. Comp. Eng.*, vol. 17, no. 1, pp. 11–23, 1992.

[15] B. R. Bean, B. A. Cahoon, C. A. Samson, and G. D. Thayer, "A world atlas of radio refractivity," Monograph 1, U.S. Dept. Commerce, Washington, DC, 1966.

[16] CCIR Recommendation 453-3, "The radio refractive index: its formula and refractivity data," in *CCIR Recomm. RPN Ser. Int. Telecommun. Union*, Geneva, Switzerland, 1992, pp. 173–180.

[17] T. Tjelta, "Prediction of multipath fading distribution on terrestrial microwave links," presented at *XXIIth Gen. Assembly URSI*, Prague, Czechoslovakia, Sept. 1990, (see pub. Lecture TF F13/90, Telenor Res. Develop., Kjeller, Norway).

[18] Recommendation ITU-R P.311-7, "Acquisition, presentation and analysis of data in studies of tropospheric propagation," ITU-R Recomm. 1994 PN Ser., *Vol. Propagat. Nonionized Media Int. Telecommun. Union*, Geneva, Switzerland, 1995, pp. 10–52, ISBN 92-61-05271-1.

[19] Recommendation ITU-R P.530-5, "Propagation data and prediction methods required for the design of terrestrial line-of-sight systems," ITU-R Recommendations 1994 PN Ser., *Vol. Propagat. Nonionized Media, Int. Telecommun. Union*, Geneva, Switzerland, 1995, pp. 297–318, ISBN 92-61-05271-1.

[20] CCIR Recommendation 530-4, "Propagation data and prediction methods required for the design of terrestrial line-of-sight systems," CCIR Recommendations, RPN Ser., *Int. Telecommun. Union*, Geneva, Switzerland, pp. 214–236, 1992.

[21] T. Tjelta and T. Tanem, "Measured and predicted enhancement on line-of-sight microwaves links," in *URSI Commun. F Open Symp.*, Ravencar, U.K., June 1992, pp. 9.1.1–6 (preprints).

[22] R. L. Olsen, L. Martin, and T. Tjelta, "A review of the role of surface reflection in multipath propagation over line-of-sight terrestrial microwave links," *NATO/AGARD Conf. Proc. Nat. Tech. Inform. Service*, Springfield, VA, Nov. 1987, no. CP-407, pp. 2/1–23.

[23] R. L. Olsen, "The role of atmospheric stratification and surface effects in multipath propagation over terrestrial line-of-sight links: A review of some recent results," in *Proc. SBMO Int. Microwave Symp.*, Sao Paulo, Brazil, July 1989, pp. 401–408.

[24] T. Tjelta, R. L. Olsen, and L. Martin, "An investigation of terrain related variables for predicting the multipath fade depth distribution on terrestrial microwave links," in *NATO/AGARD Conf. Proc. Nat. Tech. Inform. Service*, Springfield, VA, Nov. 1987, no. CP-407, pp. 1/1–9.

[25] CCIR Recommendation 581-2, "The concept of worst month," ITU-R Recommendations, 1994 PN Series, *Vol. Propagation Nonionized Media Int. Telecommun. Union*, Geneva, Switzerland, 1995, p. 248.

[26] B. Segal and R. E. Barrington, "The radio climatology of Canada: Tropospheric refractivity atlas for Canada," *Commun. Res. Ctr., Dept. Indust.*, Ottawa, Canada, CRC Rep. no. 1315, Dec. 1977.

[27] T. Tjelta and R. L. Olsen, "A data base for development and testing of worldwide techniques for predicting the multipath fading distribution on terrestrial line-of-sight links," Telenor Res. Develop., Kjeller, Norway, Rep. FoU no. 44/96, pp. 131, Nov. 1996.

[28] R. L. O. Tattersal and N. E. Cartwright, "Multipath propagation data collected from tests on line-of-sight radio paths at 11, 20, 37 GHz during the period 1972–1975," P.O. Res. Dept. Rep. 594, British Telecom Res. Lab., Martlesham Heath, U.K., Feb. 21, 1977.

[29] U. Casiraghi, S. Ciccotti, G. Ettorre, and L. Ordano, "Deep fade occurrence factor in Italy: Considerations on the available prediction formulae on the basis of 40 years of experimental results," in *Proc. Eur. Conf. Radio Relay Syst.*, Paris, France, Dec. 1991, pp. 293–300.

[30] T. Ooi and K. Morita, "Estimation formula for Rayleigh fading and equivalent Rayleigh fading occurrence probabilities," *Rev. Elec. Commun. Lab.*, vol. 51, pp. 51–57, Jan./Feb. 1981 (Japan).

[31] ITU-R Doc. 5C/GREY/5 (Canada/Norway), "Proposed revisions to Recommendation 530-3," *Int. Telecommun. Union*, Geneva, Switzerland, Oct. 1993 (reprod. Appendix I, Doc. 3M/13, Sept. 1994).

[32] C. Bilodeau, "Measurements of UHF radio propagation on the baffin and labrador coasts," *Commun. Res. Ctr., Dept. Commun.*, Ottawa, Canada, CRC Rep. no. 1430, July 1988.

[33] J. I. Strickland, R. L. Olsen, and H. L. Werstiuk, "Measurements of low-angle fading in the Canadian Arctic," *Ann. Télécommunic.*, vol. 32, pp. 530–535, Nov./Dec. 1977.

[34] R. L. Olsen and T. Tjelta, "Modeling of coastal and overwater multipath fading distributions," in *Proc. URSI Comm. F Workshop "Climatic Parameters Radiowave Propagat."*, Oslo, Norway, June 1996, pp. 24–25.

[35] CCIR Recommendation 452-5, "Prediction procedure for the evaluation of microwave interference between stations on the surface of the Earth at frequencies above about 0.7 GHz," CCIR Recommendations, RPN Ser. Int. *Telecommun. Union*, Geneva, Switzerland, pp. 285–317, 1992.

[36] ITU-R Doc. 3M/52 (Canada/Norway), "Proposed revisions to Recommendation ITU-R P.530-6, Methods for Predicting Multipath Fading Distributions in the Average Worst Month," in *Int. Telecommun. Union*, Geneva, Switzerland, Dec. 1996.

[37] Recommendation ITU-R 530-7, "Propagation data and prediction methods required for the design of terrestrial line-of-sight systems," *Int. Telecommun. Union*, vol. 1997, P. Ser., Pt. 2, pp. 271–295, 1997.

[38] K. H. Craig, T. Tjelta, and B. Segal, "Climatic parameters in clear-air propagation modeling," in *URSI Comm. F Open Symp. "Climatic Parameters Radiowave Propagat."*, Moscow, Russia, May/June 1994, pp. 8.2.1–6 (preprints).

[39] T. Tjelta, "Modeling line-of-sight worst month multipath occurrence as function of basic link and geoclimatic variables," in *Proc. URSI Comm. F Workshop "Climatic Parameters Radiowave Propagat."*, Oslo, Norway, June 1996, pp. 22–23.



**Roderic L. Olsen** (S'65–M'70) was born in Saskatoon, Saskatchewan, Canada, on December 31, 1941. He received the B.A.Sc. and the Ph.D. degrees in electrical engineering from the University of British Columbia, Vancouver, BC, Canada, in 1965 and 1970, respectively.

Since 1970, he has been employed as a Research Scientist at the Communications Research Centre (CRC) in Ottawa. His work has been primarily in the area of tropospheric propagation effects on terrestrial and earth-space communications at centimeter and millimeter wavelengths. He currently manages the VHF-EHF Propagation Group at CRC, which is carrying out research on a wide range of propagation effects on both terrestrial and earth-space links. He was a Visiting Scientist at the Centre National d'Études des Télécommunications (CNET), Lannion, France, between 1983 and 1985.

Dr. Olsen is currently Canadian National Chairman of Commission F of the International Scientific Radio Union. He has been a delegate to various meetings of the International Telecommunications Union (ITU) since 1977, and has been responsible for terrestrial line-of-sight and transhorizon propagation within the Radiocommunications Sector of the ITU (formerly the International Radio Consultative Committee–CCIR) since 1983. He has also been active in various IEEE activities in the past and served as Chairman of the Ottawa Section in 1981/1982.



**Terje Tjelta** received the M.Sc. degree in physics from the University of Bergen, Norway, in 1980, and the Ph.D. degree from University of Tromsø, Norway, in 1997.

In 1980, he joined Telenor Research and Development and has remained there except for one year (1984/1985) when he was a Visiting Researcher at "Centre Nationale d'Études des Télécommunications" (CNET), France. He has mostly been engaged in research on tropospheric radiowave propagation, in particular, clear-air effects on radiocommunications systems. He has experience from and still participates in several international cooperative research projects and activities for the International Telecommunication Union.